Gold Nanoparticles Decorated with Oligo(ethylene glycol) Thiols: Protein Resistance and Colloidal Stability†

Fajun Zhang,‡ Maximilian W. A. Skoda,‡,§ Robert M. J. Jacobs,⊥ Stefan Zorn,‡ Richard A. Martin,|| Christopher M. Martin,# Graham F. Clark,# Günter Goerigk,+ and Frank Schreiber*,‡

Institut für Angewandte Physik, Universität Tübingen, Auf der Morgenstelle 10, D-72076 Tübingen, Germany, Physical and Theoretical Chemistry Laboratory, University of Oxford, South Parks Road, Oxford, OX1 3QZ, United Kingdom, Chemistry Research Laboratory, University of Oxford, 12 Mansfield Road, Oxford, OX1 3TA, United Kingdom, Department of Physics, University of Bath, Bath BA2 7AY, United Kingdom, Synchrotron Radiation Source (SRS), Daresbury Laboratory, Warrington, Cheshire, WA4 4AD, United Kingdom, and Institut für Festkörperforschung, Forschungszentrum Jülich, Postfach 1913, D-52425, Germany

Received: June 4, 2007; In Final Form: July 24, 2007

The interactions between proteins and gold colloids functionalized with protein-resistant oligo(ethylene glycol) (OEG) thiol, $HS(CH_2)_{11}(OCH_2CH_2)_6OMe$ (EG6OMe), in aqueous solution have been studied by small-angle X-ray scattering (SAXS) and UV−vis spectroscopy. The mean size, 2*R*, and the size distribution of the decorated gold colloids have been characterized by SAXS. The monolayer-protected gold colloids have no correlations due to the low volume fraction in solution and are stable in a wide range of temperatures (5−70 °C), pH (1.3−12.4), and ionic strength (0−1.0 M). In contrast, protein (bovine serum albumin) solutions with concentrations in the range of 60−200 mg/mL (4.6−14.5 vol %) show a pronounced correlation peak in SAXS, which results from the repulsive electrostatic interaction between charged proteins. These protein interactions show significant dependence on ionic strength, as would be expected for an electrostatic interaction (Zhang et al. *J. Phys. Chem. B* **2007**, *111*, 251). For a mixture of proteins and gold colloids, the protein−protein interaction changes little upon mixing with OEG-decorated gold colloids. In contrast, the colloid−colloid interaction is found to be strongly dependent on the protein concentration and the size of the colloid itself. Adding protein to a colloidal solution results in an attractive depletion interaction between functionalized gold colloids, and above a critical protein concentration, c*, the colloids form aggregates and flocculate. Adding salt to such mixtures enhances the depletion effect and decreases the critical protein concentration. The aggregation is a reversible process (i.e., diluting the solution leads to dissolution of aggregates). The results also indicate that the charge of the OEG self-assembled monolayer at a curved interface has a rather limited effect on the colloidal stabilization and the repulsive interaction with proteins.

1. Introduction

Self-assembly of thiols on various solid substrates provides a convenient method to tailor the interfacial properties of metals, metal oxides, and semiconductors.[1−5] While initially alkanethiols and other simple thiols were in focus, the attention later shifted toward more complex self-assembled monolayers (SAMs) with functional properties.[1−8] Among these properties, the protein resistance of oligo(ethylene glycol) (OEG) SAMs has attracted much attention in recent years because of the numerous applications in biotechnology and medical devices.[9−23] The majority of these studies has been performed on flat surfaces, whereas little is known about curved surfaces.[24] On flat surfaces, systematic studies suggest that many factors are involved in the protein resistance at the OEG/water interface. For example, the factors discussed for OEG thiols themselves are packing density,[9,10] thiol composition,[11,12] internal hydrophilicity, and terminal hydrophilicity,[13] while environmental factors such as the hydration layer of the SAM,[14−16] pH, or ionic strength[17,18] have also been claimed to be important.

One of the important fundamental issues related to the mechanism of protein resistance of OEG SAMs is obviously the determination of the effective interaction between the SAM and the protein in solution. Feldman et al.[19] observed an electrostatic, long-ranged repulsive interaction with fibrinogen-functionalized AFM tips on approach to OEG-grafted gold substrates. This repulsive potential is thought to arise from a tightly bound layer of hydroxide ions, which preferably penetrate into the SAM and create a net negative electrostatic potential,[20] which then acts against the also negatively charged protein molecules. Very recent results of Skoda et al. indicate a rather strong interaction of OEG SAMs with water and the penetration of water into the SAM.[25] Using surface force spectroscopy, Dicke and Hähner also observed similar long-ranged repulsive interaction that strongly depends on the ionic strength and pH of the solution.[17,18] On the other hand, a recent molecular

† Part of the "Giacinto Scoles Festschrift".

* Corresponding author. Telephone: ++49-7071-29-78663. Fax: ++49-7071-29-5110. E-mail: frank.schreiber@uni-tuebingen.de.
‡ Universität Tübingen.
§ Physical and Theoretical Chemistry Laboratory, University of Oxford.
⊥ Chemistry Research Laboratory, University of Oxford.
|| University of Bath.
Daresbury Laboratory.
+ Forschungszentrum Jülich.

10.1021/jp074293v CCC: $37.00
Published on Web 10/03/2007

simulation study indicated a much shorter-ranged repulsive interaction.[21] In addition, it also claimed that the total interfacial forces mainly come from hydration water, while the surface charge or electrostatic interaction has a very minor part to play in the interaction.[21] Overall, the mechanism of protein resistance of OEG SAMs is still not fully understood.

Studies on curved surfaces (i.e., protein interactions with OEG-decorated gold colloids), on the other hand, may help elucidate the mechanism of their protein resistance. It is known that the phase behavior of colloids in solution depends strongly on the interactions.[26] It has long been known that a short-ranged attractive potential plays an important role in colloidal systems.[27,28] Recent progress has led to many new observations, such as liquid−liquid phase separation and the formation of dynamic glass states.[29−33] A recent study by Stradner et al. indicates that the combination of short-range attraction and long-range repulsion can lead to the formation of small equilibrium clusters in protein solutions and binary colloidal and polymer solutions.[34] The short-range attraction can be raised by mixing colloids with different size or adding nonabsorption polymer in colloidal solution, creating a "depletion" effect.[35−44] Many works have been done both theoretically and experimentally (see recent reviews, refs 35−37). It has been shown that the depletion effect in a mixture of colloids of different sizes strongly depends on the interactions between the various components.[35−44] A more complicated condition (i.e., the phase behavior of colloidal rod−sphere mixtures) has been studied in Lekkerkerker's group.[38−41] Their theoretical model predicted that a colloidal fluid to crystal phase transition can occur at very low concentration of added colloidal rods, which has been confirmed by subsequent experimental investigation.

When mixing protein with OEG-decorated colloid, the phase behavior of the mixtures should provide insight into the mechanism of the protein resistance of OEG SAMs. Zheng et al.[24] successfully synthesized OEG-protected gold colloids with average size about 3 nm. By using gel electrophoresis, protein binding to OEG-protected gold colloids was examined. It was concluded that the OEG-protected gold colloids do not bind to either the basic protein lysozyme or the acidic protein bovine serum albumin (BSA). Despite the importance of such studies, only a few studies involving curved interfaces have been published to date. It is known that directly synthesized alkanethiol-protected gold colloids are limited in size of 1−10 nm.[45−49] Larger functionalized colloids have to be prepared by a second chemisorption process.[45] Therefore, work needs to be done to understand the effective interactions in such a complex system and the effects of curvature on the conformation of molecules in the SAM, which has been already reported to be important in the protein resistance of the OEG SAM.[10,11] In addition, the stability of such functionalized gold colloids is also important for their various applications.[1−3,50−52]

In this article, we present a comprehensive study of the interactions between gold colloids, coated with $HS(CH_2)_{11}(OCH_2CH_2)_6OMe$ SAMs, abbreviated EG6OMe, and BSA. We used EG6OMe-functionalized gold colloids with different diameters as a template for surfaces with varying curvature instead of flat gold substrates. The complex systems composed of solutions of functionalized gold colloids and proteins were studied by small-angle X-ray scattering (SAXS) and UV−vis spectroscopy. On a more fundamental level, our study provides insight into the interaction potentials of colloidal mixtures and addresses important issues such as the boundary conditions for the stability of such mixtures. The studied system can also serve as a model that allows the observation of very subtle interactions, such as short-range depletion forces between the protein-resistant colloids and the proteins in solution.

2. Experimental Section

2.1. Materials. Citrate-stabilized gold colloids with various diameters were purchased from British BioCell International (BBI) and Sigma-Aldrich and were used as received. Hexa(ethylene glycol)-terminated thiol, $HS(CH_2)_{11}(OCH_2CH_2)_6OMe$, was purchased from ProChimia and was used as received. BSA (product no. A7638) was purchased from Sigma-Aldrich. This is a lyophilized powder with a molecular weight of ∼66 kDa and was used as received. Protein concentrations were determined by UV absorption based on absorption at wavelengths of 410 and 280 nm. The extinction coefficient of BSA at 280 nm is 39020/M/cm, or 0.5912/(mg/mL)/cm, calculated from the amino acid sequence.[53]

2.2. Preparation of Surface-Modified Gold Colloids. Monodispersed gold colloids with various diameters were modified by directly adding 0.1 mg/mL of EG6OMe to the colloid solution. This corresponds to an excess of EG6OMe by a factor between 10^2 and10^3 based on a simple calculation considering the total surface area of gold colloids and the cross section of the thiol molecule. Weisbecker et al.[54] reported detailed studies on the stability of various aliphatic thiols on gold colloids. They found that although alkanethiols with $HS(CH_2)_nR$, R = CH_3, OH, or CO_2CH_3, lead to fast flocculation, oligo(ethylene glycol) thiols with $HS(CH_2)_{11}(OCH_2CH_2)_yOH$, $y > 3$, stabilize the gold colloids. After the modified colloids were incubated at room temperature for more than 4 h, the stability of the modified colloids was examined by monitoring the UV−vis spectra when varying pH, ionic strength, and temperature. The modified gold colloids are stable in the experimental conditions to temperature (5−70 °C), NaCl concentration (0−1.0 M), and pH (1.3−12.4).

2.3. Methods. *2.3.1. UV−Visible Spectroscopy.* UV−visible absorption and kinetic measurements were performed at room temperature using a Cary 50 UV−visible spectrophotometer (Varian Optical Spectroscopy Instruments). Quartz cuvettes or disposable PE UV cuvettes with an optical path length through the sample of 1.0 cm were used to contain the sample while collecting the spectra in the wavelength range from 300 to 800 nm.

2.3.2. Small-Angle X-ray Scattering. SAXS measurements were carried out at station 6.2 of the Synchrotron Radiation Source (SRS) at the Daresbury Laboratory, Warrington, U.K.[55] The beam energy was 15.0 keV, corresponding to a wavelength of 0.827 Å. The scattered intensity was registered with a 200-mm radius quadrant detector located 3.3 m from the sample. The accessible q-range was thus from 0.013 to 0.45 $Å^{-1}$. The detector response was calibrated using the scattering from water. The angular scale was calibrated using the scattering peaks of silver behenate.

A sample cell with two mica windows (25-μm thick) separated by a 1.0-mm Teflon spacer was filled with protein solutions. To calculate the absolute intensity, the empty cell and salt solutions were also measured. All measurements were carried out at room temperature. The resulting data were (electronically) converted to a 1D profile by being integrated around an arc. The raw data were corrected for transmission, fluctuation of primary beam intensity, exposure time, and geometry of the detector. The detailed data correction and calibration have been described in a previous publication.[56]

Additional SAXS measurements (Table 1, Figures 2 and 5b) were performed at the JUSIFA beamline at HASYLAB/DESY,

TABLE 1: Gold Colloids Used in This Work and Related Parameters Determined by SAXS

AuEG6OMe	source	particles/mL[a]	mean size $2R$ (Å)	width of size distribution	volume fraction(s) ($\times 10^{-9}$)	critical concn of BSA (mg/mL)
Au9EG	BBI	5.7×10^{12}	94.6	0.87	1.34	>500
Au19EG	BBI	7×10^{11}	188/108	1.58/9.74	1.22/0.32	380−400[b] 320−350[c] 280−310[d] 280−310[e]
Au22EG	Sigma		219	1.23	0.5	180−200
Au37EG	BBI	9×10^{11}	369/287	2.2/5.8	0.54/0.94	60−80

[a] Numbers obtained from online product catalog http://www.bb-international.com/research.htm. [b−e] These values correspond to NaCl concentrations of 0.0, 0.1, 0.3, and 0.5 M, respectively.

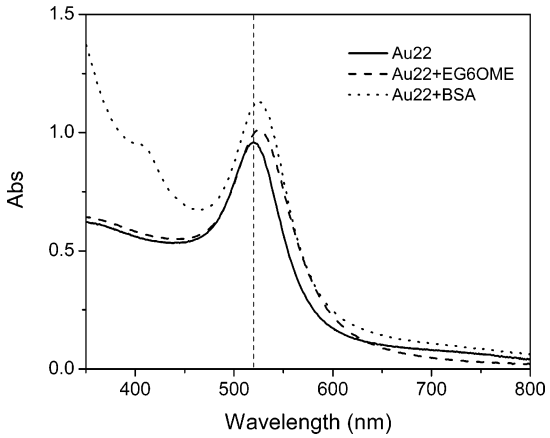

Figure 1. UV−vis spectra of gold colloid solution with $2R = 218$ Å before and after decoration by EG6OMe. For comparison, a spectrum of colloid solution with BSA is also shown.

Hamburg,[57] in the energy range of 11.7−17.5 keV. A q range from 0.0075 to 0.28 Å^{-1} was covered. The samples, as well as the buffer solution, were filled into capillaries from Hilgenberg GmbH. The capillaries were made of borosilicate glass with an inner diameter of 4.0 mm and a wall thickness of 50 μm. The capillaries were glued into custom-made aluminum holders, and these holders were sealed at both ends by O-rings and M6 screws. The scattering of water or a salt solution was measured as the background, in exactly the same way as the protein/colloidal solutions, and was subtracted from the sample scattering.

3. Results and Discussion

This section is organized as follows. First, we present the characterization of OEG-decorated gold colloids. Second, we present the influence of ionic strength on the stability of OEG-decorated gold colloids and the protein−protein interactions in solution. Last and most significantly, we discuss the phase behavior of the mixtures as a function of protein concentration and ionic strength.

3.1. Characterization of OEG-Decorated Gold Colloids. The citrate-stabilized gold colloids with a diameter of >5 nm show a characteristic absorption peak at a wavelength of ~520 nm in the UV−vis spectra. Upon decoration with EG6OMe, the reaction is characterized by a clear peak shift to a higher wavelength (524 nm). Figure 1 presents typical UV−vis spectra of a gold colloid solution (22 nm) before and after OEG decoration. As a comparison, a spectrum of the citrate-stabilized colloid solution mixed with 200 mg/mL of BSA is also shown in Figure 1. A clear shift of about 4 nm indicates the absorption of BSA molecules at the negatively charged colloid surface.[58] Both OEG SAM and absorbed BSA layer stabilize the gold colloidal solutions.

The number density of the colloidal solution is ~10^{12} particles/mL (Table 1), which corresponds to a volume fraction less than 0.003 vol %. The colloid with OEG SAM can be described by a core−shell form factor. However, because of the very large contrast, that is, difference in X-ray scattering length density between gold ($\rho_{Au} = 130.5 \times 10^{10}$ cm^{-2}) and OEG SAM ($\rho_{OEG} = 7.293 \times 10^{10}$ cm^{-2}), the contribution of the SAM to the total scattering intensity is very small. Therefore, the data analysis was carried out using a standard model (i.e., simple sphere, neglecting the shell) and least-square fitting. The total scattering intensity in a polydispersed and dilute colloidal solution with homogeneous electron density is given by:[59−61]

$$I(q) = N_0 \Delta\rho \int_0^\infty f(R) R^6 P^2(qR)\, \mathrm{d}R \qquad (1)$$

where N_0 is the number of the colloidal particles per unit volume and $\Delta\rho$ is the difference in scattering length densities between colloid and solvent (water). $f(R)$ is the normalized Gaussian distribution function:

$$f(R) = \frac{1}{\delta\sqrt{2\pi}} \exp\left[-\frac{1}{2\delta^2}(R - R_{avg})^2\right] \qquad (2)$$

where R_{avg} is the average radius as determined in the data fitting procedure and δ is the standard deviation that corresponds to the width of the size distribution. $P(qR)$ is the form factor of a spherical colloid:

$$P(qR) = \frac{3[\sin(qR) - qR\cos(qR)]}{(qR)^3} \qquad (3)$$

Data fitting was performed using Irena SAS modeling macros for Igor Pro developed by Ilavsky.[59] Figure 2 displays the SAXS experimental data with model fitted data for two sizes of gold colloids. The mean sizes of gold colloids after decoration were characterized by small-angle X-ray scattering as listed in Table 1. The experimental data can be very well fitted by the theoretical model. The size distribution gives a major component close to the size as provided by the manufacturer. Note that the gold colloids labeled as 20 nm purchased from BBI show a mean size of 18.9 nm, while colloids from Sigma-Aldrich give a mean size of 21.8 nm. We will make use of this difference later in this article.

3.2. Effect of Ionic Strength (NaCl) on Functionalized Colloidal Gold and Protein Solution. OEG-decorated colloidal gold solutions are very stable against variations of the ionic strength. Figure 3a shows a set of SAXS data for Au22EG with various salt concentrations (offset for clarity). The scattering profiles are identical, indicating that salt does not affect the stability of gold colloids in this regime. This observation indicates that the stabilization of gold colloid by OEG SAM is

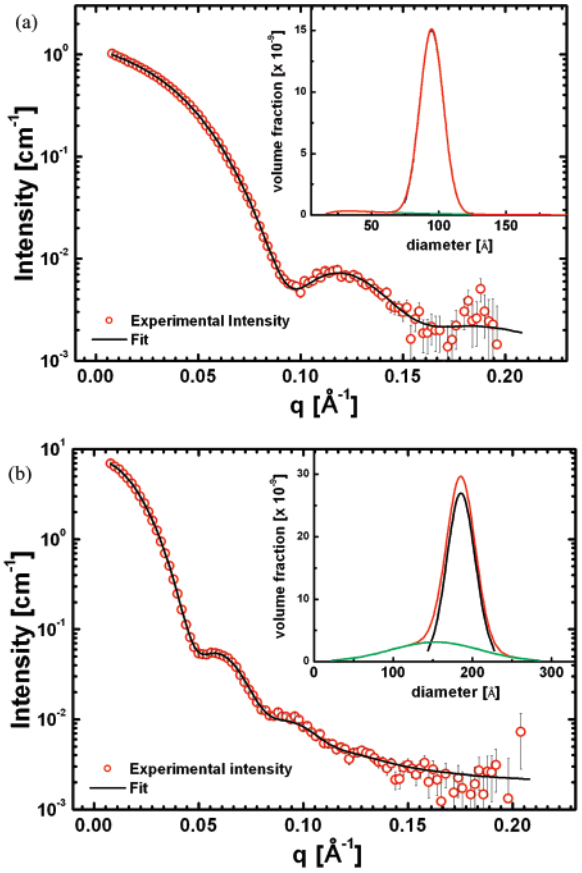

Figure 2. Experimental scattering intensity with model fitting of EG6OMe-decorated gold colloids studied by SAXS: (a) Au9EG and (b) Au19EG. Data as well as Au37EG were fitted by a bimodal size distribution. Fitting results are summarized in Table 1.

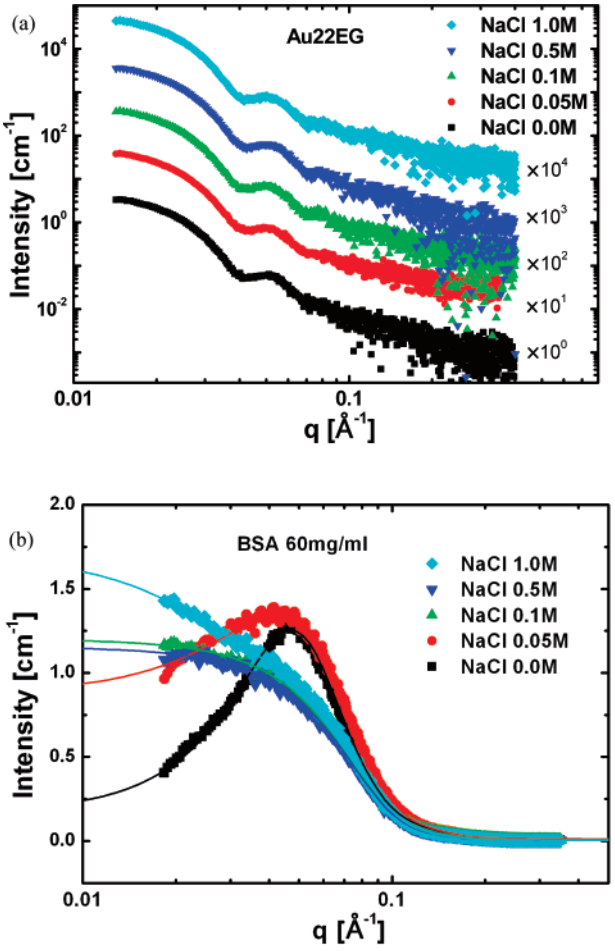

Figure 3. Effect of salt concentration on (a) Au22EG solution (offset for clarity) and (b) BSA solution of 60 mg/mL characterized by SAXS.

mainly due to entropic effects, rather than to the absorbed surface charge. Entropic effects are actually quite plausible considering that the SAM is unlikely to be a crystalline, full-coverage layer (see Section 4.2). The observations are in good agreement with the results reported by Weisbecker et al.[54] who found that OEG-decorated gold colloids are stable in a wide range of ionic strengths and pH values.

In contrast to OEG-decorated gold colloidal solutions that show a good stability against salt, protein interactions strongly depend on the ionic strength and have been intensively studied by SAXS.[33,34,56,62−69] In a previous study,[56] we have shown that the electrostatic interaction dominates the repulsive interaction between negatively charged BSA molecules in aqueous solution. With added salt, the surface charges are increasingly screened, and at very high salt concentration (>1.0 M), an attractive interaction arises due to the excluded-volume effect of ions. Figure 3b shows one example for protein concentrations of 60 mg/mL at various salt concentrations. The overall interaction at low salt concentration is repulsive and turns into a weak attractive interaction at high salt concentration.[56]

3.3. Interaction of Proteins with Functionalized Gold Colloids in Mixture Solutions. *3.3.1. SAXS Measurements.* Figure 4 presents the scattering profiles of Au22EG with different amounts of protein. For comparison, the SAXS profiles from pure colloidal and pure protein solutions are also presented. The scattering from the pure colloidal solution has been described in Figure 2. The data can be fitted by a sphere form factor with a Gaussian distribution. The scattered intensity increases significantly toward the origin. The scattering profiles from pure protein solution show a maximum intensity at finite q values (i.e., q_{max} = 0.048, 0.055, and 0.066 Å^{-1} for protein solutions of 60, 100, and 200 mg/mL, respectively). The scattering profiles from the mixtures show the combined features: a significant increase of intensity with decreasing q in low q range (<0.03 Å^{-1}), which is the typical feature of scattering from the pure colloidal solution, and a scattering maximum which almost overlaps with the scattering profile from the pure protein solution in the high q range (>0.03 Å^{-1}). While the scattering intensity distribution from the mixtures in the high q range (protein regime >0.03 Å^{-1}) almost completely follows the scattering intensity of the pure protein solution, the overall scattering intensity at low q range decreases with increasing protein concentration, which is only partially due to the increased protein concentration. When the protein concentration is above a critical protein concentration (i.e., 200 mg/mL), a new sharp scattering maximum appears at q = 0.0267 Å^{-1}. Figure 4b shows the SAXS results of a protein−colloidal mixture with 0.5 M NaCl. Similar results were obtained for salt concentrations from 0.05 to 1.0 M (data not shown). As shown in Figure 3, adding salt does not affect the scattering intensity distribution of pure colloidal solution, whereas for protein solutions it does. Nevertheless, at large q the total scattering profiles of the mixtures still qualitatively follow the features of the scattering profile of the pure protein solution. A new peak again appears at q = 0.0267 Å^{-1} at a protein concentration of 200 mg/mL (Figure 4b).

Figure 5 shows the SAXS profiles of Au22EG and Au19EG, respectively, upon adding protein above the critical protein concentration, c*. For Au22EG with 200 mg/mL of BSA, a new peak appears at a low q = 0.0267 Å^{-1}, which corresponds

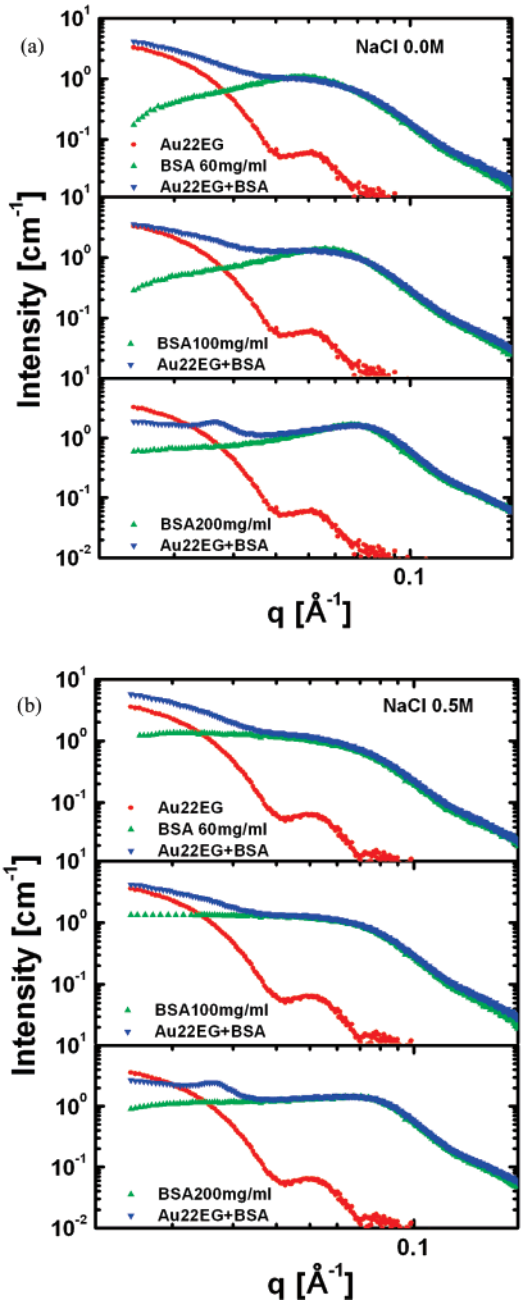

Figure 4. Mixture of OEG-coated gold colloids and protein solutions studied by SAXS. (a) SAXS profiles of Au22EG solutions with different BSA concentrations without salt. (b) SAXS profiles of Au22EG plus BSA with 0.5 M NaCl. For comparison, the SAXS data from pure colloidal solution and pure protein solution are also presented.

to a center-to-center distance of 236 Å, and the peak position does not change with added salt (Figure 5a). For Au19EG, no new peak is observed when the protein concentration is less than 300 mg/mL. Figure 5b shows that, at 400 mg/mL, a sharp peak appears at $q = 0.0316$ Å $^{-1}$, corresponding to a center-to-center distance of 199 Å. The difference between the center-to-center distance and the averaged mean size of gold colloids is mostly due to the finite thickness of the OEG SAM, but because of the spread of the experimental values, it is difficult to determine the thickness of the SAM precisely. Moreover, it can be expected that the SAM exhibits some conformational distortions and also not necessarily full coverage. Its effective thickness will thus be below the theoretical maximum value of ~29 Å (the length of the solvated EG6Me molecules in a closely packed SAM without tilting).[70] Hence, even allowing for

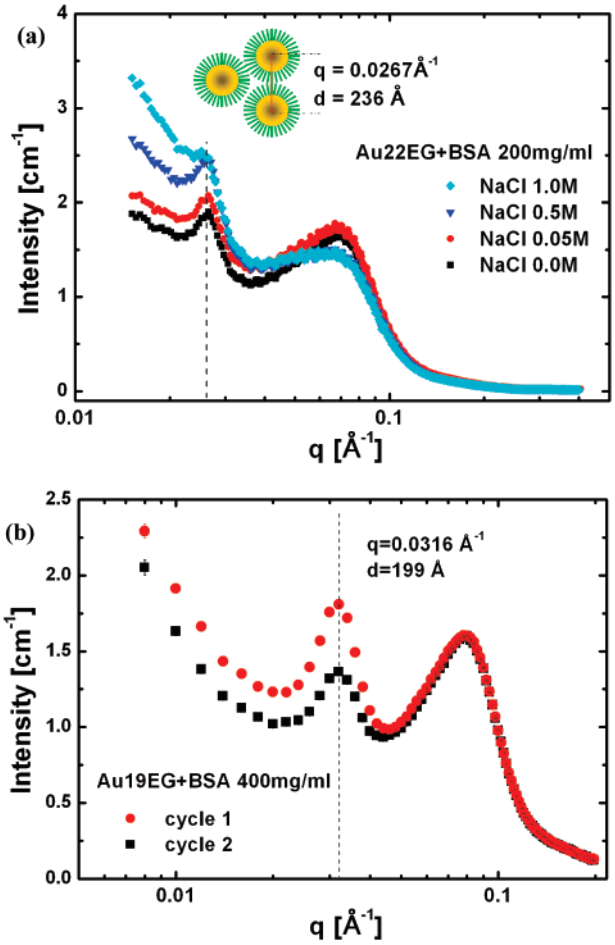

Figure 5. (a) SAXS results of Au22EG and BSA 200 mg/mL with various salt concentrations. For Au22EG solution, when BSA concentration was 200 mg/mL, colloids form aggregates and a sharp peak at $q = 0.0267$ Å $^{-1}$ corresponding to an interparticle distance of 236 Å was observed in the SAXS profile. (b) SAXS result of Au19EG with BSA 400 mg/mL. Aggregation was observed for protein concentrations >350 mg/mL. The peak position $q = 0.0316$ Å^{-1} corresponds to an interparticle distance of 199 Å.

significant experimental error, it is likely that the conformation of OEG molecules at a curved interface is greatly disturbed by the curvature. It is expected that the smaller the size of colloid, and hence the larger the curvature of interface, the greater the disorder of the OEG SAM.

We note here that the SAXS measurements for protein−colloid mixtures usually commenced about 1 or 2 h after the sample was prepared. From UV−vis measurements (see section 3.3.2), it is clear that for Au22EG with 200 mg/mL of BSA, it takes several hours until the colloids precipitate out. The time window of the SAXS measurements is thus in the intermediate stage of the aggregate formation in solution. Two consecutive cycles measured on a time scale of 30 min for Au19EG with 400 mg/mL of BSA in Figure 5b show a decrease in the intensity of the correlation peak, indicating the precipitation of colloidal clusters. It is important to note that the peak position remained constant. However, the kinetics strongly depends on the size of colloids and protein concentration. In another case, Au37EG with 100 mg/mL of BSA, most of the colloids had precipitated when the measurements started, and only the scattering intensity from proteins was observed (data not shown). More detailed studies of the kinetics of the aggregation are beyond the scope of this article and will be discussed elsewhere.[71]

3.3.2. UV−Vis Spectroscopy Observations. UV−vis spectroscopy has been used to determine the critical protein

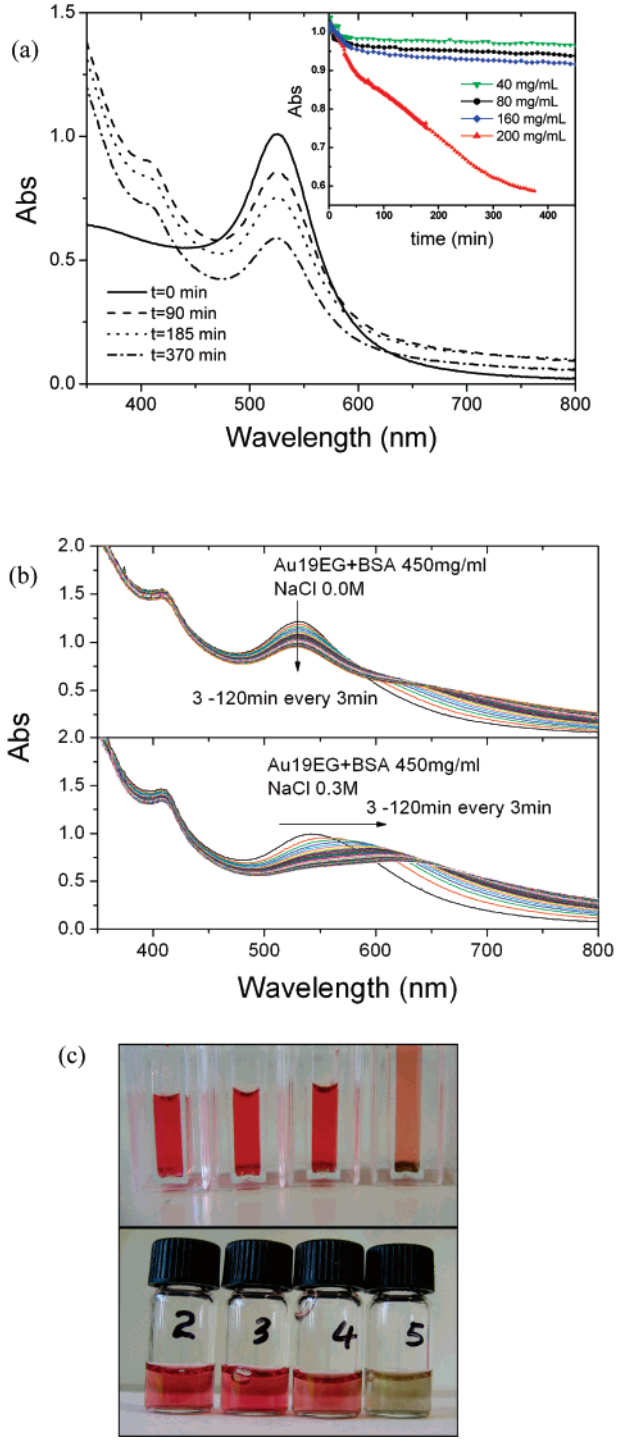

Figure 6. Real-time UV−vis spectra for (a) Au22EG with BSA 200 mg/mL (inset shows the peak intensity at 525 nm as a function of time with BSA concentration of 40, 80, 160 and 200 mg/mL); (b) Au19EG with BSA at ionic strength of 0.0 and 0.3 M; and (c) colorimetric results of Au22EG (top) (conditions are the same as those in Figure 6a) and Au19EG solution (bottom) at ionic strength of 0.3 M with BSA concentrations of 180, 220, 270, and 310 mg/mL. Critical concentration in the range of 270−310 mg/mL was determined.

concentration in various colloidal solutions. Figure 6a presents selected in situ UV−vis spectra of Au22EG solutions with a BSA concentration of 200 mg/mL. While the peak intensity decreases with time, its position stays constant. When proteins with a concentration of less than 200 mg/mL are added, the peak position still remains constant but the peak intensity at wavelength of 525 nm decreases slightly. The peak intensity as a function of time has been plotted in the inset of Figure 6a with various BSA concentrations. The peak intensities decrease in arbitrary units from 1.00 to 0.95, 0.92, and 0.89 for protein concentrations of 0, 40, 80, and 160 mg/mL, respectively. The slight decrease of absorbance is due to the diluting effect of adding powder protein to the solutions. Once the protein concentration is equal to or higher than 200 mg/mL, the peak intensity decreases continuously from 1.00 to less than 0.6 within 400 min and the peak position does not change in this time period. This continuous decrease cannot be explained by the diluting effect; rather, it is due to the aggregation and flocculation of EG6OMe-decorated gold colloids.[54,72] The UV−vis spectra in Figure 6a show that the peak intensity decreases dramatically, and at the same time, the intensity in the wavelength range of 600−800 nm increases with time. This is characteristic of aggregate formation in such a system.[54,72]

A color change from pink to yellow corresponding to the UV−vis spectra has been shown in Figure 6c (top) when the BSA concentration increased from 40 to 200 mg/mL. In addition, after several hours, some black precipitates could be observed at the bottom of the cuvette. These precipitates are large aggregates of colloids. In contrast to the irreversible aggregation upon chemisorption of alkanethiols,[54,73] it is interesting to see that the aggregates can be redispersed by diluting the solution with water, and the color changes back to pink again.

The critical protein concentration, c*, for various colloidal solutions has also been determined. For a given colloidal number density (Table 1), it is found that the critical protein concentration is very sensitive to the size of colloids. For example, c* for Au22EG is around 200 mg/mL, while for Au37EG, this value is only 50−70 mg/mL. For a slightly smaller colloid, Au19EG, c* increases to ~350 mg/mL. For Au9.3EG, we did not see any obvious color or UV−vis spectra change up to 500 mg/mL of BSA.

We have also studied the effects of ionic strength on colloid aggregation. Figure 6b shows typical UV−vis spectra for Au19EG with 450 mg/mL of BSA with and without added salt. Without salt, the peak position remains constant and the intensity decreases continuously as seen in Figure 6a. When salt is added (0.3 M NaCl), the peak not only decreases in intensity, but also shows a strong red shift. The color of the solution changes from pink to dark blue within 10 min, indicating the formation of large colloidal clusters (Figure 6c bottom). After more than 4 h, the aggregates precipitate out and the solution becomes yellow, the color of the BSA solution. Note that, in both cases, the aggregation process is reversible (i.e., diluting the solution by adding water leads to dissolution of the aggregates and the solution becomes pink again). A detailed analysis of the change in kinetics upon adding salt in the mixtures is beyond the scope of this article and will be addressed in detail elsewhere.[71] Here, we only note the decrease of critical protein concentration upon adding salt. For example, for the same Au19EG colloidal solution, without adding salt, c* is 380−400 mg/mL, and with 0.1 and 0.3 M NaCl, the c* is reduced to 320−350 and 280−310 mg/mL, respectively (Table 1 and Figure 6c lower part), c* does not change significantly upon further increasing salt concentration to 0.5 M.

4. Discussion of the Interactions in Mixed Solutions

4.1. Depletion Effect in Mixed Colloidal Systems. Generally, interactions are translated into correlations between particles, which then enter the structure factor measured in small-angle scattering. Interactions in *mixed* dispersions are related to the *partial structure* factors. In binary mixtures (i.e., protein

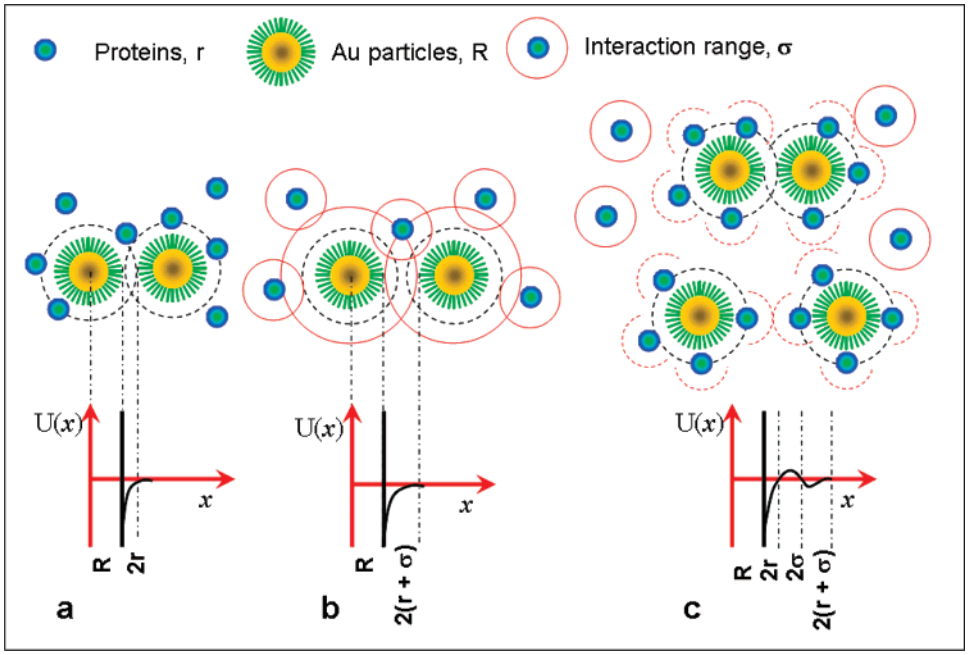

Figure 7. Schematic drawing of depletion interaction under various conditions. (a) Both particles are hard spheres, and the depletion interaction has a range of $2r$. (b) Both particles have an external repulsive potential with interaction range σ. The effective interaction between big particles is an enhanced depletion interaction with a range of $2(r + \sigma)$. (c) Small particles have an external repulsive potential of σ, while big particles are hard spheres. The effective interaction between a pair of big particles shows an "oscillation" potential.[35] When adding salt to this solution, the external Coulombic repulsion is screened, and the whole system is back to the condition of Figure 7a. Note that the scattering data cannot be directly converted, so that the potentials presented here serve as a good model, but they are not necessarily the unique model. For detailed description, see text.

and functionalized gold colloidal solution), the partial structure factors are protein−protein interaction $S_{pp}(q)$, colloid−colloid interaction $S_{cc}(q)$, and protein−colloid interaction $S_{pc}(q)$. Partial structure factors are usually determined by small-angle neutron scattering with a contrast matching technique.[43,44,74−79] For the theoretical calculation of partial structure factors, the detailed interactions of all components need to be known. In our case, the structure factor of colloid−colloid interactions in the pure colloidal solution can be approximated to be equal to unity because of the very low volume fraction. The protein−protein interactions in pure protein solutions have been reported in ref 56 and can be described by a screened Coulombic structure factor at low salt concentration and a square-well structure factor with attractive potential at very high salt concentration. The protein−colloid interaction is not known, but it may be reasonable to expect a short-ranged repulsive potential (see later discussion on ionic strength effect).

In mixtures, the interactions can change. While the protein−protein interactions in the mixtures do not change very much, as shown in SAXS measurements (Figure 4 and 5), the colloid−colloid interactions change with increasing protein concentration. The formation of colloidal aggregates above a critical protein concentration indicates that the addition of proteins results in an effective attraction between colloids. The attractive interaction between gold nanoparticles can be understood by the depletion effect.[27,28,35−44] The attractive potential induced by the depletion effect in the case of binary mixtures of hard spheres is given by[27,38−41]

$$U(h) = -3k_BT\phi_s \frac{R}{2r}\left(1 - \frac{h}{2r}\right)^2 \qquad (4)$$

Here, k_BT is the thermal energy, ϕ_s is the volume fraction of the small spheres, R and r are the radii of the large and small particles, respectively, and h is the distance between the surfaces of the two large spheres. The center-to-center interparticle distance, D, is equal to $h + 2R$.

The depletion interaction under various conditions is presented schematically in Figure 7.[35,36] In a mixture of hard spheres with two different sizes (Figure 7a), small particles are expelled from the "forbidden region" between two large particles. This depletion effect leads to an unbalanced osmotic pressure pushing the large particles together, which results in an effective attraction between the two large particles. This attraction potential depends on the size ratio ($\lambda = r/R$) between small and large particles and their volume fraction.[35−44] From eq 4, we can see that a decrease of λ or an increase in the volume fraction of the small particle increases the strength of the depletion potential. In our experiments, we indeed observed the enhanced depletion effect (i.e., the decrease of c*; Table 1) with increasing size of colloid.

The depletion effect in our system is more complicated than for a mixture of hard spheres because of the electrostatic repulsive interaction between proteins, which results in a strong ionic strength dependence of the colloidal stability. The following scenario is similar to what was discussed by Belloni.[35] When both particles have an external repulsive potential with interaction range σ (Figure 7b), the effective interaction between large particles is an enhanced depletion interaction with a range of $2(r + \sigma)$. If the small particles have an external repulsive potential of σ, while the big particles are hard spheres (Figure 7c), then the interaction between small and big particles is still effectively a hard sphere interaction. Because protein molecules repel each other through a long-range repulsion of a range $\sigma \gg 2r$, they tend to accumulate near inert colloidal surfaces. The dashed half circle around them indicates the repulsive interaction to other small particles. When the interparticle distance, D, of a pair of big particles is such that $2R < D < 2R + 2r$, a depletion interaction similar to that in Figure 7a occurs. If the interparticle distance is increased, $2R + 2r < D < 2R + 2r + 2\sigma$, the

repulsion between the accumulation layer creates a repulsive zone with a range of 2σ; further increasing the distance, $2R + 2r + 2\sigma < D < 2R + 2r + 2\sigma + 2(r + \sigma)$, leads to a depletion interaction similar to that in Figure 7b. Therefore, the effective interaction between a pair of big particles shows an "oscillation" potential that is damped out very fast.[35] When adding salt to this solution, the external Coulombic repulsion is screened, and the whole system reverts back to the condition of Figure 7a.

4.2. Effect of Ionic Strength. Generally, UV−vis spectra indicate that adding salt (which reduces the Debye length) to the mixtures decreases the critical protein concentration (Table 1) and also speeds up the aggregation (Figure 6b). Upon adding salt directly into the colloidal solution, we find that the spectra do not change at all (data not shown). Interactions between the OEG-decorated gold colloids include attractive van der Waals forces, which is the major reason for the flocculation of colloidal solutions. If there are no repulsive interactions to balance the van der Waals forces, the gold colloids will aggregate.[54] In the case of OEG-decorated gold colloids in solution, the repulsive interactions may arise from surface charge (i.e., negative charge due to the tightly bound layer of hydroxide ions)[17−20] or the steric or entropic effect of the OEG SAM layers. Our experimental results indicate that the resulting colloidal solutions are stable at ionic strengths up to 1.0 M. In this case, the surface charge is completely screened. In contrast, native, citrate-stabilized colloidal gold is very sensitive to ionic strength and aggregates quickly upon addition of salt. Therefore, it can be concluded that it is not the surface charge that is responsible for nonaggregation of the colloids.

In the mixture of colloid and protein, the protein molecules are negatively charged; if the colloidal surface is also negatively charged, then the electrostatic repulsive interaction will enhance the depletion effect in solution (Figure 7b).[35] Upon adding salt, we screened the surface charges, and the depletion effect will be relatively reduced. This contradicts our experimental observation; when adding salt, we observed an enhanced depletion effect: a faster aggregation of colloid or lower critical protein concentration. This observation also contradicts the idea of the existence of a significant surface charge on the colloidal surface.

Hence, the repulsive interaction in a colloidal solution is more likely to originate mainly from the entropic effects of the OEG SAM layer, which is a rather short-ranged interaction of the order of the thickness of the hydration layer. The interaction between colloid and protein is also related to this short-ranged repulsive interaction. Compared to the long-ranged repulsive interaction between protein molecules, the colloid is rather "neutral" to the protein molecules. In this case, an oscillatory structure force arises, which reduces the depletion effect (Figure 7c caption).[35,36] Because protein molecules repel each other through a long-range repulsion of a range $\sigma \gg 2r$, they tend to accumulate near inert colloidal surfaces and a repulsion at contact followed by oscillations will appear at high protein density in the colloid−colloid effective potential.[35] When salt of less than 0.3 M is added, the surface charges of proteins are progressively screened, the oscillation effect is reduced, and c* decreases. For salt concentrations higher than 0.3 M, the surface charge is severely screened and adding more salt does not change the effective interaction significantly, as shown in Table 1.

5. Conclusions

On the basis of the results and discussion presented in this article, we reach the following conclusions. First, OEG SAMs stabilize colloidal gold in solution in a wide range of temperature, ionic strength and pH. In addition, such OEG-protected gold colloids do not bind to protein, indicating the protein resistance of the OEG SAM. Second, the interactions between protected colloid and protein in mixtures, which determine the mechanism of protein resistance of the OEG SAM, show a rather short-ranged, possibly mainly entropic repulsive contribution. Third, the decorated colloids can form aggregates upon adding protein above a critical concentration, c*. The aggregates can be redissolved by diluting the solution. Our results demonstrate that adding proteins to such a colloidal solution ($2R > 100$ Å) creates an attractive depletion interaction between colloids. This depletion effect is enhanced with increasing size of colloids because of the enhanced imbalance of osmotic pressure. A decrease of c* was observed by using a larger size of colloid. The effective interaction between colloids also depends on the ionic strength of the solution as observed by the decrease of c* upon increasing the ionic strength. This effect of ionic strength is explained as screening of the surface charge of proteins, which changes the interaction potential between colloids from an "oscillatory" potential to a pure depletion attractive potential as schematically presented in Figure 7.

Acknowledgment. We thank the reviewers of the manuscript for very constructive suggestions. We gratefully acknowledge financial support from the Engineering and Physical Sciences Research Council (EPSRC) and the CCLRC for the allocation of beamtime on MPW 6.2 at the SRS, Daresbury, U.K. Some of the SAXS measurements were carried out at JUSIFA beamline at HASYLAB, DESY, Hamburg, Germany.

References and Notes

(1) Ulman, A. *Chem. Rev.* **1996**, *96*, 1533.
(2) Mrksich, M.; Whitesides, G. M. *Annu. Rev. Biophys. Biomol. Struct.* **1996**, *25*, 55.
(3) Love, J. C.; Estroff, L. A.; Kriebel, J. K.; Nuzzo, R. G.; Whitesides, G. M. *Chem. Rev.* **2005**, *105*, 1103.
(4) Schreiber, F. *Prog. Surf. Sci.* **2000**, *65*, 151.
(5) Schreiber, F. *J. Phys.: Condens. Matter* **2004**, *16*, R881.
(6) Fenter, P.; Eisenberger, P.; Liang, K. S. *Phys. Rev. Lett.* **1993**, *70*, 2447.
(7) Schreiber, F.; Eberhardt, A.; Leung, T. Y. B.; Schwartz, P.; Wetterer, S. M.; Lavrich, D. J.; Berman, L.; Fenter, P.; Eisenberger, P.; Scoles, G. *Phys. Rev. B* **1998**, *57*, 12476.
(8) Chidsey, C. E. D.; Liu, G.-Y.; Rowntree, P.; Scoles, G. *J. Chem. Phys.* **1989**, *91*, 4421.
(9) Vanderah, D. J.; La, H.; Naff, J.; Silin, V.; Rubinson, K. A. *J. Am. Chem. Soc.* **2004**, *126*, 13639.
(10) Zheng, J.; Li, L.; Chen, S.; Jiang, S. *Langmuir* **2004**, *20*, 8931.
(11) Li, L.; Chen, S.; Zheng, J.; Ratner, B. D.; Jiang, S. *J. Phys. Chem. B* **2005**, *109*, 2934.
(12) Balamurugan, S.; Ista, L. K.; Yan, J.; López, G. P.; Fick, J.; Himmelhaus, M.; Grunze, M. *J. Am. Chem. Soc.* **2005**, *127*, 14548.
(13) Herrwerth, S.; Eck, W.; Reinhardt, S.; Grunze, M. *J. Am. Chem. Soc.* **2003**, *125*, 9359.
(14) Kreuzer, H. J.; Wang, R. L. C.; Grunze, M. *J. Am. Chem. Soc.* **2003**, *125*, 8384.
(15) Pertsin, A. J.; Hayashi, T.; Grunze, M. *J. Phys. Chem. B* **2002**, *106*, 12274.
(16) Pertsin, A. J.; Grunze, M. *Langmuir* **2000**, *16*, 8829.
(17) Dicke, C.; Hähner, G. *J. Am. Chem. Soc.* **2002**, *124*, 12619.
(18) Dicke, C.; Hähner, G. *J. Phys. Chem. B* **2002**, *106*, 4450.
(19) Feldman, K.; Hähner, G.; Spencer, N. D.; Harder, P.; Grunze, M. *J. Am. Chem. Soc.* **1999**, *121*, 10134.
(20) Zolk, M.; Eisert, F.; Pipper, J.; Herrwerth, S.; Eck, W.; Buck, M.; Grunze, M. *Langmuir* **2000**, *16*, 5849.
(21) Zheng, J.; Li, L.; Tsao, H.-K.; Sheng, Y.; Chen, S.; Jiang, S. *Biophys. J.* **2005**, *89*, 158.
(22) Yu, J. J.; Tan, Y. H.; Li, X.; Kuo, P. K.; Liu, G. Y. *J. Am. Chem. Soc.* **2006**, *128*, 11574.
(23) Wang, R. L. C.; Kreuzer, H.; Grunze, M. *Phys. Chem. Chem. Phys.* **2000**, *2*, 3613.
(24) Zheng, M.; Davidson, F.; Huang, X. *J. Am. Chem. Soc.* **2003**, *125*, 7790.

(25) Skoda, M. W. A.; Jacobs, R. M. J.; Willis, J.; Schreiber, F. *Langmuir* **2007**, *23*, 970.
(26) Witten, T. A.; Pincus, P. A. *Structured Fluids: Polymers, Colloids, Surfactants;* Oxford University Press: New York, 2004.
(27) Asakura, S.; Oosawa, F. *J. Chem. Phys.* **1954**, *22*, 1255.
(28) Verduin, H.; Dhont, J. K. G. *J. Colloid Interface Sci.* **1995**, *172*, 425.
(29) Trappe, V.; Prasad, V.; Cipelletti, L.; Segre, P. N.; Weitz, D. A. *Nature* **2001**, *411*, 772.
(30) Pham, K. N.; Puertas, A. M.; Bergenholtz, J.; Egelhaaf, S. U.; Moussaïd, A.; Pusey, P. N.; Schofield, A. B.; Cates, M. E.; Fuchs, M.; Poon, W. C. K. *Science* **2002**, *296*, 104.
(31) Eckert, T.; Bartsch, E. *Phys. Rev. Lett.* **2002**, *89*, 125701.
(32) Sciortino, F. *Nat. Mater.* **2002**, *1*, 145.
(33) Sciortino, F.; Mossa, S.; Zaccarelli, E.; Tartaglia, P. *Phys. Rev. Lett.* **2004**, *93*, 055701.
(34) Stradner, A.; Sedgwick, H.; Cardinaux, F.; Poon, W. C. K.; Egelhaaf, S. U.; Schurtenberger, P. *Nature* **2004**, *432*, 492.
(35) Belloni, L. *J. Phys.: Condens. Matter* **2000**, *12*, R549.
(36) Likos, C. N. *Phys. Rep.* **2001**, *348*, 267.
(37) Poon, W. C. K. *J. Phys.: Condens. Matter* **2002**, *14*, R859.
(38) Vliegenthart, G. A.; Lekkerkerker, H. N. W. *J. Chem. Phys.* **1999**, *111*, 4153.
(39) Koenderink, G. H.; Vliegenthart, G. A.; Kluijtmans, S. G. J. M.; van Blaaderen, A.; Philipse, A. P.; Lekkerkerker, H. N. W. *Langmuir* **1999**, *15*, 4693.
(40) Vliegenthart, G. A.; van Blaaderen, A.; Lekkerkerker, H. N. W. *Faraday Discuss.* **1999**, *112*, 173.
(41) Mao, Y.; Cates, M. E.; Lekkerkerker, H. N. W. *Physica A* **1995**, *222*, 10.
(42) Ye, X.; Narayanan, T.; Tong, P.; Huang, J. S. *Phys. Rev. Lett.* **1996**, *76*, 4640.
(43) Ye, X.; Narayanan, T.; Tong, P.; Huang, J. S.; Lin, M. Y.; Carvalho, B. L.; Fetters, L. J. *Phys. Rev. E* **1996**, *54*, 6500.
(44) Dijkstra, M.; Roij, R.; Evans, R. *Phys. Rev. E* **1999**, *59*, 5744.
(45) Aslan, K.; Pérez-Luna, V. H. *Langmuir* **2002**, *18*, 6059.
(46) Shon, Y. S.; Mazzitelli, C.; Murray, R. W. *Langmuir* **2001**, *17*, 7735.
(47) Aguila, A.; Murry, R. W. *Langmuir* **2000**, *16*, 5949.
(48) Kometani, N.; Tsubonishi, M.; Fujita, T.; Asami, K.; Yonezawa, Y. *Langmuir* **2001**, *17*, 578.
(49) Templeton, A. C.; Chen, S.; Gross, S. M.; Murray, R. W. *J. Phys. Chem. B* **2000**, *104*, 564.
(50) Rosi, N. L.; Mirkin, C. A. *Chem. Rev.* **2005**, *105*, 1547.
(51) Daniel, M. C.; Astruc, D. *Chem. Rev.* **2004**, *104*, 293.
(52) Raschke, G.; Kowarik, S.; Franzl, T.; Sönnichsen, C.; Klar, T. A.; Feldmann, J.; Nichtl, A.; Kurzinger, K. *Nano Lett.* **2003**, *3*, 935.
(53) Kozak, M. *J. Appl. Crystallogr.* **2005**, *38*, 555.
(54) Weisbecker, C. S.; Merritt, M. V.; Whitesides, G. M. *Langmuir* **1996**, *12*, 3763.
(55) Cernik, R. J.; Barnes, P.; Bushnell-Wye, G.; Dent, A. J.; Diakun, G. P.; Flaherty, J. V.; Greaves, G. N.; Heeley, E. L.; Helsby, W.; Jacques, S. D. M.; Kay, J.; Rayment, T.; Ryan, A.; Tang, C. C.; Terrill, N. J. *J. Synchrotron Radiat.* **2004**, *11*, 163.
(56) Zhang, F.; Skoda, M. W. A.; Jacobs, R. M. J.; Martin, R. A.; Martin, C. M.; Schreiber, F. *J. Phys. Chem. B* **2007**, *111*, 251.
(57) Haubold, H. G.; Gruenhagen, K.; Wagener, M.; Jungbluth, H.; Heer, H.; Pfeil, A.; Rongen, H.; Brandenberg, G.; Moeller, R.; Matzerath, J.; Hiller, P.; Halling, H. *Rev. Sci. Instrum.* **1989**, *60*, 1943.
(58) Brewer, S. H.; Glomm, W. R.; Johnson, M. C.; Knag, M. K.; Franzen, S. *Langmuir* **2005**, *21*, 9303.
(59) Irena 2 package of SAS data evaluation and modeling macros for Igor Pro. http://www.uni.aps.anl.gov/~ilavsky/irena.html (accessed June, 2006).
(60) Kotlarchyk, M.; Chen, S. H. *J. Chem. Phys.* **1983**, *79*, 2461.
(61) Kline, S. R. *J. Appl. Crystallogr.* **2006**, *39*, 895.
(62) Cinelli, S.; Spinozzi, F.; Itri, R.; Finet, S.; Carsughi, F.; Onori, G.; Mariani, P. *Biophys. J.* **2001**, *81*, 3522.
(63) Spinozzi, F.; Maccioni, E.; Teixeira, C. V.; Amenitsch, H.; Favilla, R.; Goldoni, M.; Muro, P. D.; Salvato, B.; Mariani, P.; Beltramini, M. *Biophys. J.* **2003**, *85*, 2661.
(64) Tardieu, A.; Le Verge, A.; Malfois, M.; Bonneté, F.; Finet, S.; Riès-Kautt, M.; Belloni, L. *J. Cryst. Growth* **1999**, *196*, 193.
(65) Narayanan, J.; Liu, X. Y. *Biophys. J.* **2003**, *84*, 523.
(66) Velev, O. D.; Kaler, E. W.; Lenhoff, A. M. *Biophys. J.* **1998**, *75*, 2682.
(67) Malfois, M.; Bonneté, F.; Belloni, L.; Tardieu, A. *J. Chem. Phys.* **1996**, *105*, 3290.
(68) Petsev, D. N.; Vekilov, P. G. *Phys. Rev. Lett.* **2000**, *84*, 1339.
(69) Liu, Y.; Fratini, E.; Baglioni, P.; Chen, W. R.; Chen, S. H. *Phys. Rev. Lett.* **2005**, *95*, 118102.
(70) Schwendel, D.; Hayashi, T.; Dahint, R.; Pertsin, A.; Grunze, M.; Steitz, R.; Schreiber, F. *Langmuir* **2003**, *19*, 2284.
(71) Zhang, F.; Skoda, M. W. A.; Jacobs, R. M. J.; Zorn, S.; Martin, R. A.; Martin, C. M.; Schreiber, F. Manuscript in preparation.
(72) Lazarides, A. A.; Schatz, G. C. *J. Phys. Chem. B* **2000**, *104*, 460.
(73) Mayya, K. S.; Patil, V.; Sastry, M. *Langmuir* **1997**, *13*, 3944.
(74) Hanley, H. J. M.; Straty, G. C.; Lindner, P. *Langmuir* **1994**, *10*, 72.
(75) Ottewill, R. H.; Hanley, H. J. M.; Rennie, A. R.; Straty, G. C. *Langmuir* **1995**, *11*, 3757.
(76) Lutterbach, N.; Versmold, H.; Reus, V.; Belloni, L.; Zemb, Th.; Lindner, P. *Langmuir* **1999**, *15*, 345.
(77) Ramsay, D. F.; Avery, R. G.; Benest, L. *Faraday Discuss. Chem. Soc.* **1983**, *76*, 53.
(78) Ramsay, D. F.; Booth, B. O. *J. Chem. Soc., Faraday Trans. 1* **1983**, *79*, 173.
(79) Paula, F. L. O.; Aquino, R.; da Silva, G. J.; Depeyrot, J.; Tourinho, F. A.; Fossum, J. O.; Knudsen, K. D. *J. Appl. Crystallogr.* **2007**, *40*, s269.